

Papers published in *Hydrology and Earth System Sciences Discussions* are under open-access review for the journal *Hydrology and Earth System Sciences*

# Impacts of changes in vegetation cover on soil water heat coupling in an alpine meadow, Qinghai-Tibet Plateau, China

W. Genxu<sup>1,2</sup>, H. Hongchang<sup>2</sup>, L. Yuanshou<sup>2</sup>, and W. Yibo<sup>3</sup>

<sup>1</sup>Institute of Mountain Hazards and Environment, Chinese Academy of Sciences, Chengdu, People's Republic of China

<sup>2</sup>College of Resources and Environment, Lanzhou University, Lanzhou 730000, People's Republic of China

<sup>3</sup>Cold and Arid Regions Environmental and Engineering Research Institute, Chinese Academy of Sciences, Lanzhou, People's Republic of China

Received: 4 August 2008 – Accepted: 15 August 2008 – Published: 4 September 2008

Correspondence to: W. Genxu (gxwang@ns.lzb.ac.cn)

Published by Copernicus Publications on behalf of the European Geosciences Union.

**HESSD**

5, 2543–2579, 2008

**Impacts of vegetation cover on soil water heat regime**

W. Genxu et al.

Title Page

Abstract

Introduction

Conclusions

References

Tables

Figures

◀

▶

◀

▶

Back

Close

Full Screen / Esc

Printer-friendly Version

Interactive Discussion



## Abstract

Alpine meadow is one of the most widespread grassland types in the permafrost regions of the Qinghai-Tibet Plateau. The transmission of coupled soil water heat is one of the most important processes influencing cyclic variations in the hydrology of frozen soil regions, especially under conditions of changing vegetation cover. The present study assesses the impact of changes in vegetation cover on the coupling of soil water and heat in a permafrost region. Soil moisture ( $\theta_v$ ), soil temperature ( $T_s$ ), soil heat content, and differences in  $\theta_v-T_s$  coupling were monitored on a seasonal and daily basis under three different densities of vegetation cover (30, 65, and 93%) upon both thawed and frozen soils. Regression analysis of  $\theta_v$  vs.  $T_s$  plots under different levels of vegetation cover indicates that soil freeze-thaw processes were significantly affected by changes in vegetation cover. With decreasing vegetation cover upon an alpine meadow, the difference between air temperature and ground temperature ( $\Delta T_{a-s}$ ) also decreased. A decrease in vegetation cover also resulted in a decrease in the  $T_s$  at which soil froze and an increase in the temperature at which it thawed; this was reflected in a greater response of soil temperature to changes in air temperature ( $T_a$ ). For  $\Delta T_{a-s}$  outside the range of  $-0.1$  to  $1.0^\circ\text{C}$ , root zone soil-water temperatures showed a significant increase with increasing  $\Delta T_{a-s}$ ; however, the magnitude of this relationship was dampened with increasing vegetation cover. At the time of maximum water content in the thawing season, the soil temperature decreased with increasing vegetation. Changes in vegetation cover also led to variations in  $\theta_v-T_s$  coupling. With increasing vegetation cover, the surface heat flux increased, along with the amplitude of its variations. Soil heat storage at 20 cm depth also increased with increasing vegetation cover, and the downward transmitted of heat flux decreased. In addition to providing insulation against soil warming, vegetation in alpine meadows within the permafrost region also slows down the response of permafrost to climatic warming via the greater water-holding capacity of its root zone. Such vegetation may therefore play an important role in conserving water in alpine meadows and maintaining the stability of engineering

HESSD

5, 2543–2579, 2008

### Impacts of vegetation cover on soil water heat regime

W. Genxu et al.

Title Page

Abstract

Introduction

Conclusions

References

Tables

Figures

◀

▶

◀

▶

Back

Close

Full Screen / Esc

Printer-friendly Version

Interactive Discussion



works constructed within frozen soil of the Qinghai-Tibet Plateau.

## 1 Introduction

Global climate change has had a significant effect upon natural ecosystems in many regions of the world. Cold, high-altitude environments within alpine or high-latitude regions, in which freeze-thaw cycles lead to temporal variations in the quantity of soil water and the heat that it bears, are termed frost or permafrost ecosystems (Wu et al., 2002; Walker et al., 2003). The frost ecosystems are arguably among the most sensitive to climate change owing to the sensitivity of the permafrost environment to warming (Walker et al., 2003; Christensen et al., 2004). Changes in vegetation cover of these ecosystems lead to dramatic changes in the physical properties of soil, the dynamics of surface soil water, and the soil carbon cycle, which in turn exert a profound influence on the entire biosphere (Weller et al., 1995; Jorgenson et al., 2001; Christensen et al., 2004). Given the magnitudes of the heat sinks within frost regions, the terrestrial ecosystems of cold regions exert a strong influence on the water cycle and heat balance of regional land-atmosphere systems (Carey and Woo, 1999; Rouse, 2000). Consequently, the energy and water balance of the Qinghai-Tibet Plateau has an important influence on the Asian monsoon system, making it an important component of the energy and water cycles of the global climate (Zhang et al., 2003). Accordingly, a significant response of the alpine frost ecosystems upon the Qinghai-Tibet Plateau to global climate change would have an important feedback effect on global climate.

Shifts in energy and water balance occasioned by a response of the permafrost region's alpine frost ecosystems to global climate change, would most likely be reflected in changes of moisture content and associated heat of permafrost soil. Therefore, an understanding of the laws governing variations in soil moisture and associated heat of alpine frost ecosystems is important in understanding regional variations in water cycling arising from global climate changes (Rouse, 2000; Zhang et al., 2003). There is a growing body of research into the role of permafrost in water and heat cycles, in-

**HESSD**

5, 2543–2579, 2008

### Impacts of vegetation cover on soil water heat regime

W. Genxu et al.

Title Page

Abstract

Introduction

Conclusions

References

Tables

Figures

◀

▶

◀

▶

Back

Close

Full Screen / Esc

Printer-friendly Version

Interactive Discussion



**Impacts of vegetation cover on soil water heat regime**

W. Genxu et al.

Title Page

Abstract

Introduction

Conclusions

References

Tables

Figures



Back

Close

Full Screen / Esc

Printer-friendly Version

Interactive Discussion



cluding studies on hydrological processes in the Mackenzie Global Energy and Water Cycle Experiment (Rouse, 2000) and the role of permafrost in hydrological processes within a North American subarctic wetland (Oeche et al., 2000; Carey and Woo, 1999). These investigations in subarctic Canada and Alaska found that climate change has led to an increase in the topsoil moisture content of the permafrost region (warming moister) (Jorgenson et al., 2001; Turetsky et al., 2002); however, studies in other regions (e.g., northern Alaska) have reported reduced topsoil moisture content and even drought (warming drier) (Christensen et al., 2004). Further observations and studies in different regions are required to ascertain the laws governing water cycling within the permafrost-vegetation-atmosphere system and its influence on global climate change (Bubier et al., 1999; Oeche et al., 2000; Christensen et al., 2004).

The alpine meadows that constitute the main land type of the permafrost region of the Qinghai-Tibet Plateau are located in the source areas of several large rivers, including the Yangtze and Yellow rivers, and thereby play an important role in regulating river flow and the productivity of local grazing grasslands (Zhou, 2001; Wang et al., 2001a). The past 30 years has seen a 24% decline in the extent of high-coverage (vegetation cover in excess of 85%) alpine meadows in this region, representing a serious degradation of these ecosystems (Wang et al., 2004; Yang et al., 2005). Consequently, the purpose of the present study is to document the basic characteristics of changes in the water and heat dynamics that occur under different degrees of cover degradation in alpine meadows of the permafrost region, and to analyze the possible effects of the vegetation within alpine meadows on the region's hydrological cycle.

**2 Study area**

The current study area is the watershed of the Zuomao Kong River, a second-order tributary of the Yangtze River located in the eastern permafrost region of the Qinghai-Tibet Plateau (92° 50'–93° 3' E, 34° 40'–34° 48' N). The watershed occupies a total area of 127.63 km<sup>2</sup> at elevations ranging from 4510 to 5323 m a.s.l. (Fig. 1).

## 2.1 Vegetation and soil

Vegetation in the area is dominated by *Kobresia pygmaea* C. B. Clarke and *Kobresia humilis* Serg. According to the degree of degradation, vegetation cover in the region's grasslands is divided into three categories: non-degraded, moderately degraded, and severely degraded, corresponding to 93%, 65% and 30% coverage, respectively. In severely degraded grassland, *Kobresia sp.* is replaced by *Festuca sp.* and *Poa spp.* (Wang et al., 2001b; Zhou, 2001). Monthly average NDVI began to increase from 0.2 in late April and reached a maximum of 0.7 in August and then decreased to 0.4 in October. Consistently, Leaf area index (LAI) increased from late May and reached a maximum of 5.2 in late July and then decreased slowly (Yang et al., 2005).

Based on the data from China's second national soil survey (NSSO, 1998), the soil types in the study region were mainly classified into Mattic Cryic Cambisols (Alpine meadow soil) in Chinese taxonomy, or as Cambisols in FAO/UNESCO taxonomy, and the most significant characteristic is that there are Mattic epipedon (Oo) in Alpine meadow soil. Table 1 lists the main physical properties and nutrient contents of the region's alpine meadow soils under different levels of cover. In severely degraded alpine meadows, the amount of coarse sand and gravel within the topsoil is significantly higher than that in non-degraded areas. Soil organic matter content (SOM) in the 0–0.2 m soil layer (root zone) declines significantly with increasing degradation of vegetation cover: for a decline in cover from 93 to 30%, SOM falls from 13.6 to 4.5 g kg<sup>-1</sup>, along with a corresponding 44% reduction in total N content (Measured by us). Permafrost is well developed in the study area, averaging between 50 and 120 m in depth, with an active layer of 0.8–1.5 m and permafrost temperature of between –1.5 and –3.7°C (Zhou et al., 2000). The permafrost temperature is the annual average soil temperature measured at the depth of zero annual amplitude, and the aero amplitude depth ranged from 9.0 m to 14.0 m in the study area (Zhou et al., 2000).

HESSD

5, 2543–2579, 2008

### Impacts of vegetation cover on soil water heat regime

W. Genxu et al.

Title Page

Abstract

Introduction

Conclusions

References

Tables

Figures

◀

▶

◀

▶

Back

Close

Full Screen / Esc

Printer-friendly Version

Interactive Discussion



## 2.2 Climatic condition

The mean annual (1973–2005) air temperature ( $T_a$ ), relative humidity, and precipitation are  $-5.2^{\circ}\text{C}$ , 57%, and 310.7 mm, respectively (Zhou et al., 2000; Wang et al., 2001). Due to the summer monsoon generally occurs from May to October (Wang et al., 2001a; Yao et al., 2007), the precipitation events on the Tibetan Plateau mainly occur during the period from June to September. As shown in Fig. 2a, the precipitation in the study region mainly falls in the three months from July to September, accounting for 83% of the annual total precipitation. During the freezing season from November to April, the precipitation was less than 5 mm. The distribution of yearly air temperature has an obvious consistency with the precipitation processes, while the peak temperature occurs from July to August and the monthly average air temperature are all lower than  $0^{\circ}\text{C}$ . Monthly mean surface soil temperatures (5 cm) showed almost the same seasonal patterns as those for air temperature in an average year (Fig. 2a). The net radiation  $R_n$  was positive throughout the year-round measurement period and reached its maximum in June and July (Fig. 2b). The  $R_n$  was very high during summer compared with those in other places, such as arid regions, tropical grassland, temperate forests, Arctic tundra and boreal forest regions (Eugster et al., 2000; Yao et al., 2007). It indicated that the solar radiation resource is abundant in summer on the Tibetan Plateau.  $R_n$  was lowest in winter from December to February.

## 3 Methodology

### 3.1 Field observations of soil moisture and temperature

Three observation locations for soil water-temperature coupling (A, B, and C) were selected within the Zuomao Kong watershed, with locations A and C representing grasslands of alpine meadows and location B representing alpine frost swamp grassland (Fig. 1). At location A, we selected three  $20\times 5\text{ m}$  (slope length $\times$ width) sampling plots

## Impacts of vegetation cover on soil water heat regime

W. Genxu et al.

Title Page

Abstract

Introduction

Conclusions

References

Tables

Figures

◀

▶

◀

▶

Back

Close

Full Screen / Esc

Printer-friendly Version

Interactive Discussion



## Impacts of vegetation cover on soil water heat regime

W. Genxu et al.

Title Page

Abstract

Introduction

Conclusions

References

Tables

Figures

◀

▶

◀

▶

Back

Close

Full Screen / Esc

Printer-friendly Version

Interactive Discussion



with slopes of 18–21° and contrasting vegetation covers of 30, 65, and 93%. Two soil-moisture observation points located one-third and two-thirds of the way down the slope of each plot housed a pair of 1.5 m deep wells used for measurements of soil water and temperature. In each well, soil moisture sensors and soil temperature ( $T_s$ ) sensors were installed at depths of 0.20, 0.40, 0.70, 1.20, and 1.50 m. Before burying the water probes and temperature sensors, the soil bulk density at each point was determined using the cutting ring method. A sample sieve was used to divide the soil granularity composition into the fraction coarser than 2 mm and the fraction finer than 2 mm. The soil particle-size composition for the fraction finer than 2 mm was determined using a CIS-50 grain-size analyzer (Ankersmic Co., The Netherlands).

$\theta_v$  was the volumetric liquid water content of soil, which was determined by frequency domain reflectometry (FDR), using a calibrated soil moisture sensor equipped with a Theta-probe (Holland Eijkelamp Co.).  $\theta_v$  was derived from changes in the soil's dielectric constant, converted to a millivolt signal; the accuracy of this procedure was  $\pm 2\%$ .

$T_s$  was monitored using a thermal resistance sensor sensitive to temperature changes in the range of  $-40$  to  $50^\circ\text{C}$ , with an overall system precision of  $\pm 0.02^\circ\text{C}$ . The thermal resistance sensors were developed by the State Key Laboratory of Frozen Soil Engineering (Lanzhou, China) using digital multimeters (Fluke 180 series, Fluke Co., USA); the sensors have been successfully used upon the Qinghai-Tibet Plateau over the past 20 years (Wu et al., 2002, 2004).

Both  $\theta_v$  and  $T_s$  were monitored simultaneously at 2-h intervals from April to November and at 6 hr intervals from December to March over the 3-year period from 2004 to 2006. Two portable micro-meteorological stations were established in the experimental fields to measure the climatic factors of  $T_a$  (at 1.2 m height), precipitation, wind velocity and direction, and net radiation.

### 3.2 Analysis of changes in $\Theta_V - T_s$ coupling with vegetation cover

At present, the two methods most widely used for analyzing the soil  $\theta_V - T_s$  relationship are based on field observational data (Jansson and Karlberg, 2001; Kang et al, 2004), one is the rational method based on statistical analysis, and the other is the numerical model, known as the SHOW model method. Owing to a dearth lack of necessary data together with the difficulty of calibrating the parameters due to the lack of detail measurements, use of the latter method is impossible in this research. We analyzed the  $\theta_V - T_s$  relationship and changes in the relationship using two different approaches:

(i) using a regression model and

(ii) by analyzing the distribution of and variation in coupled soil water-heat regimes.

Using statistical methods available in SAS 8.1 (SAS Institute, 2000), we generated a regression model linking  $\theta_V$  and  $T_s$  from mean daily data collected at different soil depths and under different vegetation covers. Models developed for different levels of vegetation cover served to analyze the effects of changes in vegetation cover on the coupling of  $\theta_V$  and heat.

The effectiveness of the model was evaluated using two terms: the Nash and Sutcliffe (1970) coefficient of efficiency of the match between the simulated and observed daily soil  $\theta_V - T_s$ , and the relative error (*RE*) of soil  $\theta_V - T_s$ . The Nash-Sutcliffe coefficient of efficiency, *NSE* (Nash and Sutcliffe, 1970), is a dimensionless indicator widely used to evaluate hydrological models. *NSE* is better suited to evaluate model goodness-of-fit than the coefficient of determination,  $R^2$  (Legates and McCabe, 1999). *RE* was used to determine the fitting error of the soil  $\theta_V - T_s$  curve to observed values. *NSE* and *RE* are calculated as:

$$NSE = 1.0 - \left( \frac{\sum_{i=1}^N (O_i - P_i)^2}{\sum_{i=1}^N (O_i - \bar{O})^2} \right) \quad RE = \frac{(O_i - P_i)}{O_i} \times 100\%$$

where:  $O_i$ =measured (observed) data,  $P_i$ =modeled (predicted) data,  $\bar{O}$ =mean of measured data.

Title Page

Abstract

Introduction

Conclusions

References

Tables

Figures

◀

▶

◀

▶

Back

Close

Full Screen / Esc

Printer-friendly Version

Interactive Discussion



**Impacts of vegetation cover on soil water heat regime**

W. Genxu et al.

Title Page

Abstract

Introduction

Conclusions

References

Tables

Figures

◀

▶

◀

▶

Back

Close

Full Screen / Esc

Printer-friendly Version

Interactive Discussion



We selected soil temperature parameters closely related to  $\theta_v$ , such as soil freezing temperature ( ${}^fT_s$ ), soil thawing temperature ( ${}^tT_s$ ), soil-air temperature difference ( $\Delta T_{a-s}=T_a - T_s$ ), and soil heat content, to analyze the effects of changes in vegetation cover on coupled soil water-heat regimes. The parameters  ${}^tT_s$  and  ${}^fT_s$  were determined using the inflexion point method, based on plots of  $\theta_v$  vs.  $T_s$ . For decreasing  $T_s$ , we took  ${}^fT_s$  to be the point where  $\theta_v$  dropped sharply to a lower, relatively stable value. At this point, the simplifying assumption is made that all water is frozen except for a small residual quantity of unfrozen water. Conversely, with increasing  $T_s$  in a frozen soil, we took  ${}^tT_s$  to be the point at which the water content showed a sharp increase to a higher, relatively stable value.

For  $T_s > 0^\circ\text{C}$ , and for  $T_s < 0^\circ\text{C}$  in the case that soil water was not yet frozen,  $\theta_v$  calculated from FDR data was taken as the volumetric soil liquid-water content. For  $T_s < 0^\circ\text{C}$ , the soil water content equals the volumetric soil liquid plus the ice content, which was assumed to be the same as the liquid water content that observed the preceding fall just before the soil froze, as long as there was no significant change in the FDR data when the soil was frozen. Barring significant shifts in the FDR data, the difference in FDR data between the values of  $\theta_v$  taken at the time immediately before the soil froze and the stable values of  $\theta_v$  taken at the time of soil frozen, were taken as the volumetric soil solid-water content (Zhou et al., 2000; Zhang et al., 2003). However, it is impossible to ascertain the accuracy of the ice content due to a lack of detailed measurements. The ice content is known to change over time if the presence of a temperature gradient leads to the movement of liquid water toward the freezing front (Cheng, 1984).

For  $T_s \approx {}^fT_s$ , and when all but a small residual quantity of water is assumed to be in solid form, the soil heat content,  $E_f$ , is a function of the latent heat and sensible heat (Jansson and Karlberg, 2001; Kang et al., 2005):

$$E_f = {}^fC_s T_s - L_f W_{ic}, \tag{1}$$

where  $L_f$  is the latent heat of freezing, approximately  $334 \text{ kJ kg}^{-1}$  (Chen et al., 2006),  $W_{ic}$  is the potential freezing water content, and  ${}^fC_s$  is the soil heat capacity of frozen

soil ( $\text{kJ m}^{-3} \text{C}^{-1}$ ), as given by (Jansson and Karlberg, 2001; Chen et al., 2006)

$${}^f C_s = f_s C_s + {}^i \theta_s C_i + {}^r \theta_s C_w, \quad (2)$$

where  $C_s$  is the heat capacity of the solid soil matrix,  $C_i$  and  $C_w$  are the heat capacities of ice and liquid water, respectively,  ${}^i \theta_s$  and  ${}^r \theta_s$  are the soil ice-water content and soil residual liquid-water content, respectively, and  $f_s$  is the volumetric content of the solid soil matrix.

During the initial freezing or thawing period, the soil is in a partly frozen state; therefore, the soil heat value,  $E_t$ , can be approximated as follows (Jansson and Karlberg, 2001; Chen et al., 2006):

$$E_t = L_f w \left( \frac{T_s}{T_f} \right)^{\frac{\lambda d_3 + d_2}{d_2 d_3}} + C_i T_s, \quad (3)$$

where  $w$  is the total soil water content,  $d_2$  and  $d_3$  are empirical constants, and  $\lambda$  is the soil particle-size distribution index.

### 3.3 Determination of soil surface heat flux, including near-surface heat storage

The surface energy balance equation can be expressed as follows (Mayocchi and Bris-towa, 1995):

$$R_n - G_s - LE - H = 0 \quad (4)$$

Net radiation  $R_n$ , is measured with net radiometers, whereas the sensible heat flux ( $H$ ,  $\text{W m}^{-2} \text{s}^{-1}$ ) and the latent heat flux ( $LE$ ,  $\text{W m}^{-2} \text{s}^{-1}$ ) were calculated by using the SHAW model due to lack of observation (NWRC, 2004; Flerchinger, 2000). The soil surface heat fluxes  $G_s$ , a measure of the energy that enters (or leaves) the soil, then can be calculated by the Eq. (4).

To investigate the validity of the created SHAW model in the study region, the data of GAME/Tibet Amdo site were used to compare with the modelling results (Zhang et

Title Page

Abstract

Introduction

Conclusions

References

Tables

Figures

◀

▶

◀

▶

Back

Close

Full Screen / Esc

Printer-friendly Version

Interactive Discussion



al., 2003). The Fig. 3 showed the statistic results of calculated  $LE$  and  $G_s$  with the observed data. The results from calculation and observation were similar and their variation trends coincided. The latent heat from calculated data, to some extent, was lesser than the observed data, and the calculated soil surface heat fluxes were slightly larger than the observed data. The statistic relation coefficient  $R$  were over 0.75 and the significant level test  $P < 0.0001$  (Fig. 3), which indicate that the created SHAW model was valid and available in the study region.

### 3.4 Soil laboratory analysis

All soil samples, collected from the sampling sites of every land cover type defined, were analyzed for soil particle size, soil organic matter content and soil bulk density by standard methods (Ministry of Agriculture of China, 1993). The soil granularity was analyzed by using CIS-50 grain-size analyzer (Ankersmic Co., The Netherlands), and soil bulk density was determined simultaneously. Soil organic matter was determined by the Walkley-Black method. All determinations were replicated twice, from which a mean value was calculated for each site.

## 4 Results

### 4.1 Energy fluxes regime and its seasonal change with degree of vegetation coverage

$H$  increased with the increase of  $R_n$  from February, but started to decrease from late June, even though  $R_n$  continued to increase, reaching a lower volume in July–August when the foliage attained its maximum coverage (Fig. 4).  $H$  then began to increase again, with a second peak appearing around October.  $LE$  started to increase in late March, and the maximum value appeared in late July because the high vegetation coverage and soil water further increased  $LE$  during the growth period. When the soil froze in October, the  $LE$  became extremely small and generally lesser than  $H$  during

## Impacts of vegetation cover on soil water heat regime

W. Genxu et al.

Title Page

Abstract

Introduction

Conclusions

References

Tables

Figures

◀

▶

◀

▶

Back

Close

Full Screen / Esc

Printer-friendly Version

Interactive Discussion



winter season from November to February.  $G_s$  varied between 2.0 and  $-2.0 \text{ MJ m}^{-2}$  and reached a maximum value around June-July when the vegetation cover was relatively small and  $R_n$  was high, and then dropped below zero from terminal September (Fig. 4).

Vegetation cover variation has a significant influence on the energy flux regime. The  $H$  and  $G_s$  decreased with increasing vegetation cover (Fig. 4a and c). The annual and winter season average  $H$  under the 30% cover was exceeded those for 93% by 16% and 19%, respectively. Under the 30% cover, the  $G_s$  entered downward to deep soil from surface in warm season between June and September was more than those of 65% and 93% cover by 23.2% and 41.2%, respectively, while in winter season between October and February, the  $G_s$  overflowed upward from soil to air exceeded those of 65% and 93% cover by 17.3% and 38.1%, respectively (Fig. 4c). This implies that the lesser the vegetation cover, the more the energy was consumed to increase soil temperature and has more soil surface heat flux.

During the frozen-soil period,  $LE$  were very low with the mean value of  $0.6 \text{ MJ m}^{-2} \text{ d}^{-1}$ ,  $1.1 \text{ MJ m}^{-2} \text{ d}^{-1}$  and  $1.4 \text{ MJ m}^{-2} \text{ d}^{-1}$  for 30%, 65% and 93% cover, respectively (Fig. 4b). Most energy were converted to  $H$ , with mean  $1.6 \text{ MJ m}^{-2} \text{ d}^{-1}$ ,  $1.4 \text{ MJ m}^{-2} \text{ d}^{-1}$  and  $1.2 \text{ MJ m}^{-2} \text{ d}^{-1}$  for 30%, 65% and 93% cover, respectively. In thawing-soil period,  $LE$  rapidly increased due to the increases in precipitation and vegetation cover, and gradually became the dominant component during June and July, but  $H$  increased again after September as  $LE$  and  $G$  rapidly decreased. During the summer season from June to August, the mean  $LE$  were  $3.1 \text{ MJ m}^{-2} \text{ d}^{-1}$ ,  $4.4 \text{ MJ m}^{-2} \text{ d}^{-1}$  and  $5.9 \text{ MJ m}^{-2} \text{ d}^{-1}$ , that were 1.4 fold, 2.1 fold and 3.1 fold of the mean  $H$  value for 30%, 65% and 93% cover, respectively (Fig. 4b).

The soil heat content, represented by  $E_f$  or  $E_t$  (Eqs. 1 and 3, respectively), and its distribution throughout the soil profile were assessed under different vegetation covers during the freezing and thawing periods (Table 1). During the freezing period, the greater the value of  $\theta_v$  at freezing, and the smaller the vegetation cover, the greater the resulting  $E_f$  (Fig. 5 and Table 1). Given that the gradient in  $T_s$  with depth gave rise

## Impacts of vegetation cover on soil water heat regime

W. Genxu et al.

Title Page

Abstract

Introduction

Conclusions

References

Tables

Figures

◀

▶

◀

▶

Back

Close

Full Screen / Esc

Printer-friendly Version

Interactive Discussion



**Impacts of vegetation cover on soil water heat regime**

W. Genxu et al.

to increased accumulation of soil water in the upper active layer, the value of  $\theta_v$  in the upper 0.20–0.40 m soil layer was greater than that in the deeper layer, leading to a significantly higher value of  $E_f$  in the shallow layer. Therefore, the distribution of soil  $E_f$  and shifts in these values were the result of the combined effects of vegetation cover and initial  $\theta_v$ . During the April–June thawing of the active layer,  $E_f$  was dominated by downward transmission. At any given depth within the active layer,  $E_f$  decreased with increasing vegetation cover:  $E_f$  under 93% cover was 6.4–78.0 and 27.2–85.5% lower than that under 65 and 30% cover, respectively.

4.2 Coupling of  $\Theta_V$  and  $t_s$  and its variation with degree of vegetation coverage

Using observation data from the upper slope point, we plotted the  $\theta_v$ – $T_s$  relationship for soil freezing (Fig. 5a) and thawing (Fig. 5b) processes in the upper 0.2 m layer of alpine meadow soils under different levels of vegetation cover. For soil temperatures between entirely frozen soil ( $T_s$ ) and 5°C,  $\theta_v$  and  $T_s$  exhibited a strong correlation, regardless of the level of vegetation cover.

Based on Fig. 5, regression analysis was used to develop coupled  $\theta_v$ – $T_s$  models for periods of freezing and thawing under different levels of vegetation cover (Table 3). During the freezing process,  $\theta_v$  and  $T_s$  showed an S-shaped relationship under different levels of vegetation cover ( $R > 0.94$ ,  $P < 0.001$ , fitting  $RE < 0.45\%$ ). During the thawing process, the patterns of regression models between  $\theta_v$  and  $T_s$  were distinct from those obtained for the freezing process, under all levels of vegetation cover. Nonetheless, these  $\theta_v$ – $T_s$  relationships showed a strong correlation ( $R > 0.88$ ,  $P < 0.001$ , fitting  $RE = 2.5$ – $6.1\%$ ).

Using the observed values of  $\theta_v$ , the regression models (Table 3) were used to simulate  $T_s$  for both the freezing (Fig. 6a) and thawing (Fig. 6b) periods under different levels of vegetation cover. The simulation accuracy for the coupled  $\theta_v$ – $E_f$  was greater under low vegetation cover than under high cover. The simulation relative error  $RE$  and  $NSE$  are presented in Table 4. For the freezing process, the  $NSE$  values for the coupled  $\theta_v$ – $T_s$  model run under vegetation covers of 30, 65, and 93% were 90.3, 86.4,

Title Page

Abstract Introduction

Conclusions References

Tables Figures

◀ ▶

◀ ▶

Back Close

Full Screen / Esc

Printer-friendly Version

Interactive Discussion



and 61.3%, respectively, and the relative simulation error was in the range of 13.5 to 21%. For the thawing process, the  $NSE$  for the coupled  $\theta_v-T_s$  model exceeded 75%, and the relative error was in the range of 2.1 to 20%; i.e., better than that for the model for freezing period. As with the model for freezing period, the efficiency coefficient decreased with increasing vegetation cover. The effects of vegetation cover on the coupled  $\theta_v-T_s$  relationship are mainly manifest in the following two factors:

- (i) Soil freezing period: For a given  $\Delta T_{a-s}$ , the amplitude of the drop in  $\theta_v$  upon freezing decreased with increasing vegetation cover, while at a given soil temperature,  $\theta_v$  increased with increasing vegetation cover. The general regression model for  $\theta_v-T_s$  coupling during the freezing process can be given as

$$T_s = ST_c + A_c / [1 + \exp(\theta_0 - \theta_v) / B_c], \quad (5)$$

where  $ST_c$  and  $A_c$  are  $T_s$ -related coefficients applicable when the soil is entirely frozen and  $\theta_v$  remains stable,  $\theta_0$  is a moisture-adjustment coefficient related to the initial freezing of soil water, and  $B_c$  is the vegetation cover adjustment coefficient, inversely related to the extent of vegetation cover. Both  $ST_c$  and  $\theta_0$  are indirectly affected by changes in vegetation cover.

The essence of such a relationship lies in the fact that the different soil moisture contents under contrasting vegetation covers resulted in varying soil heat capacities and heat consumption for transformations of the water phase. For a given gradient in soil moisture, the change in soil temperature is smaller under grassland with an extensive vegetation cover than that under limited vegetation cover. However, there was a consistency phenomenon that shown from the Fig. 6 during freezing periods: the liquid water moved towards the freezing front and formed relatively high liquid water content at the soil freezing temperature caused by temperature gradient under different vegetation cover.

- (ii) Soil thawing period: From April to August (when the depth of thawing reached 1.2 m), the  $\theta_v-T_s$  relationships derived for different levels of vegetation cover

## Impacts of vegetation cover on soil water heat regime

W. Genxu et al.

Title Page

Abstract

Introduction

Conclusions

References

Tables

Figures

◀

▶

◀

▶

Back

Close

Full Screen / Esc

Printer-friendly Version

Interactive Discussion



**Impacts of vegetation cover on soil water heat regime**

W. Genxu et al.

Title Page

Abstract

Introduction

Conclusions

References

Tables

Figures



Back

Close

Full Screen / Esc

Printer-friendly Version

Interactive Discussion



showed less variation than those obtained during the freezing period. The amplitude of the increase in  $\theta_v$  with increasing  $T_s$  grew larger with decreasing vegetation cover. For soil under a vegetation cover of 93%, the liquid water content in the 0–20 cm soil layer reached a maximum value at a soil temperature of 0.2°C; under vegetation covers of 65 and 30%, it attained maximum values at 1 and 1.5–2.0°C, respectively. This implies that the lesser the vegetation cover, the more sensitive heat consumption to increase the soil temperature, and more the vegetation cover, the more latent heat consumption to transfer water phase and increase soil liquid water content.

In contrast to the freezing period, the pattern of  $\theta_v-T_s$  coupling during the thawing period showed some variation with different degrees of vegetation cover: for non-degraded or slightly degraded alpine meadow soils, a three-parameter logarithmic curve relationship provided the best fit to the data, whereas for severely degraded vegetation cover, the significance of this relationship was a single-axis hyperbolic regression model provided a better fit in this case. The main causes of different  $\theta_v-T_s$  coupling pattern were possibly the variation of energy balance and the initial ice content in the 0–20 cm soil layer under different vegetation cover. During thawing periods, the heat flux entered into soil and its transferring rate increased with vegetation cover decrease, and the latent heat consumption increased more quickly with vegetation cover increase. The different energy balance and soil water (ice) content were also the reason of the simulation accuracy variation with different degrees of vegetation cover.

Based on extensive observational and experimental data, but without taking into account the influence of vegetation cover, Xu et al. (2001) derived an experiential exponential formula of the  $\theta_v-T_s$  coupling relationship to use in describing frozen soils:  $\theta = a |T - 273.15|^{-C}$ . The basic form of this formula is similar to that for the  $\theta_v-T_s$  coupling relationship for the soil thawing process under a higher vegetation cover (see Table 3). For a given range in soil temperature, the statistical  $\theta_v-T_s$  coupling relationship during the soil freezing period (as listed in Table 3) shows a similar trend to that described by the experiential exponential formula presented above.

## 4.3 Effects of vegetation cover on the soil water-heat coupling regime

### 4.3.1 Effects of changes in vegetation cover on the soil-air temperature difference

Land-atmosphere energy exchange upon alpine meadows has an important influence on the soil water cycle. Given that surface vegetation is an intermediate step in the land-atmosphere energy transmission process, it is important to understand how changes in the pattern of vegetation cover affect this process if we are to understand the cyclic energy-transfer processes of the atmosphere-vegetation-soil system within permafrost regions.

Figure 7 shows the dynamic changes in the soil-air temperature difference under different levels of vegetation cover, as obtained from an analysis of observed soil temperatures in the top 20 cm layer of soil and surface air temperatures. During the thawing period,  $\Delta T_{a-s}$  showed a positive value, and heat was transmitted from the atmosphere to the soil. During the freezing period, the mean daily soil temperature was higher than the air temperature,  $\Delta T_{a-s}$  was dominantly negative, and heat was transmitted from the soil to the atmosphere. During the initial freezing period,  $\Delta T_{a-s}$  was small and largely invariant under different levels of vegetation cover; however, during the initial thawing period,  $\Delta T_{a-s}$  varied dramatically due to fluctuating air temperature, but showed similar trends for different levels of vegetation cover. For cases in which the soil in the 0–20 cm layer was either entirely thawed or frozen,  $\Delta T_{a-s}$  showed an increasing trend with increasing vegetation cover. During soil freezing and thawing processes,  $\Delta T_{a-s}$  showed a similar trend of dynamic variations under different levels of vegetation cover, although with contrasting amplitudes.

The  $\Delta T_{a-s} - T_s$  plots for the soil thawing period show significantly steeper slopes than those for the freezing period (Table 5). The slopes of  $\Delta T_{a-s} - T_s$  plots for 93% vegetation exceeded those for 65 and 30% cover by 3.5 and 17.4%, respectively. Similarly, the mean  $\Delta T_{a-s}$  values obtained under 93% vegetation cover exceeded those under 65 and 30% cover by 8.3 and 26.7%, respectively.

During the warm season (July 20 to September 10), the active layer soil was entirely

## Impacts of vegetation cover on soil water heat regime

W. Genxu et al.

Title Page

Abstract

Introduction

Conclusions

References

Tables

Figures

◀

▶

◀

▶

Back

Close

Full Screen / Esc

Printer-friendly Version

Interactive Discussion



**Impacts of vegetation cover on soil water heat regime**

W. Genxu et al.

Title Page

Abstract

Introduction

Conclusions

References

Tables

Figures



Back

Close

Full Screen / Esc

Printer-friendly Version

Interactive Discussion



thawed, vegetation within the alpine meadow showed rapid growth, and a significant linear relationship was observed between  $\Delta T_{a-s}$  and  $T_a$ , with values of the former extending over a greater range than that recorded during the freezing or thawing periods (Table 5). As with the freezing and thawing periods, the slopes of  $\Delta T_{a-s} - T_s$  plots for the warm season increase in steepness with increasing vegetation cover. The  $\Delta T_{a-s} - T_s$  slope for soil under 93% vegetation cover exceeded those for 65 and 30% cover by 6.9 and 15.7%, respectively. Similarly, the mean  $\Delta T_{a-s}$  values obtained under 93% cover exceeded those under 65 and 30% cover by 6.7 and 22.2%, respectively.

4.3.2 Effects of the soil-air temperature difference change on soil water content

The soil-air temperature difference change has different relationship with soil water content under different degrees of vegetation cover (Fig. 8). During periods of freezing and thawing, changes in  $\theta_v$  were similar to those for  $\Delta T_{a-s}$ ; i.e., for  $-1^\circ\text{C} < \Delta T_{a-s} < 1^\circ\text{C}$ ,  $\theta_v$  in the root zone (0–0.20 m) showed a rapid increase with increasing  $\Delta T_{a-s}$ . However, for  $\Delta T_{a-s} < -1^\circ\text{C}$  and  $1^\circ\text{C} < \Delta T_{a-s}$ , changes in  $\theta_v$  in tandem with  $\Delta T_{a-s}$  were less pronounced:  $\theta_v$  remained relatively stable. For  $T_a > 2^\circ\text{C}$ ,  $\Delta T_{a-s}$  was not evidently tied to  $\theta_v$ , and remained relatively stable. For example, for  $T_a > 2^\circ\text{C}$  and  $\Delta T_{a-s} > 1.2^\circ\text{C}$  (Fig. 8b), no correlation is observed between  $\theta_v$  and  $T_a$ ; therefore, at least in the permafrost region and within the 1.2 m of the active layer, a rise in  $T_a$  had a limited positive influence on  $\theta_v$  of the alpine meadow, and this only occurred over a certain temperature range ( $< 1^\circ\text{C}$ ). Given that  $\Delta T_{a-s}$  increases with the level of vegetation cover, the influence of changes in  $T_a$  on  $\theta_v$  within a high-cover alpine meadow (such as vegetation cover of 93%) was less pronounced for  $T_a > 2^\circ\text{C}$ .

4.3.3 Effects of vegetation cover on the freezing and thawing temperature of the active layer

Soil freezing and thawing temperatures are related to factors such as vegetation cover, soil moisture, soil salt content, and soil structure. Given that the observation points in

**Impacts of vegetation cover on soil water heat regime**

W. Genxu et al.

Title Page

Abstract

Introduction

Conclusions

References

Tables

Figures

◀

▶

◀

▶

Back

Close

Full Screen / Esc

Printer-friendly Version

Interactive Discussion



this study were all located within the same geomorphological unit and the same soil type, the soil salt contents and fine-grained composition of the soil of the different points are essentially the same (Table 1). Therefore, the effect of soil salt content on the soil water-heat regime is not relevant in this study. The data in Table 5 show that the soil freezing temperature fell with decreasing vegetation cover.

Values of  ${}^i T_s$  and  ${}^f T_s$  show a close relationship to  $\theta_v$  (Oechel et al., 2000; Zhou et al., 2000), and vary with vegetation cover (Table 5).  ${}^f T_s$  decreased with decreasing vegetation cover: under a cover of 93%, soil within the alpine meadow began to freeze at about  $-0.1^\circ\text{C}$ , whereas under moderately degraded grassland (63% cover) it began to freeze at between  $-0.7$  and  $-0.8^\circ\text{C}$ . For severely degraded alpine meadow (30% cover), values of  ${}^f T_s$  were  $1.6$  and  $1.0^\circ\text{C}$  lower than those under 63 and 93% cover, respectively.

${}^i T_s$  increased with decreasing vegetation cover. High-cover alpine meadow soil thawed entirely at approximately  $0.04^\circ\text{C}$ , whereas moderate-cover soil thawed entirely at  $0.3^\circ\text{C}$ .  ${}^i T_s$  for highly-degraded (30% cover) alpine cold meadow was  $1.7$  and  $1.3^\circ\text{C}$  higher than that for high-cover (93%) or moderate-cover (63%) soils, respectively.

Prior to mid-July, soil temperature showed marked variations under different levels of vegetation cover (Fig. 9a): mean soil temperature in the 0–20 cm layer under 30% cover was  $2.5^\circ\text{C}$  higher than that under 93% cover and  $1.3^\circ\text{C}$  higher than that under 65% cover. After mid-July, soil in the 0–20 cm layer thawed entirely, leading to a reduction in the magnitude of variation in soil temperature under different levels of vegetation cover; however, the soil temperature under 30% cover was still higher than that under more extensive cover, and we found that the higher the vegetation cover, the lower the soil temperature. During the freezing period (Fig. 9b), greater vegetation cover was associated with smaller amplitudes of soil temperature change and higher soil temperature.

## 5 Discussion

It should be noted that the factors affecting the soil water-heat relationship in the active layer are complex; in particular, the vegetation cover, snow cover, water regime, and soil structure and composition have a significant effect on the relationship (Smith and Riseborough, 1996; Wang et al., 2001a). Smith and Riseborough (1996, 2002) developed the TTOP model to analyze the effects of vegetation, snow cover, and soil properties on the temperature of permafrost. According to the theory upon which this model is based, if the effect of snow cover is absent, the vegetation cover shows a positive influence on soil temperature. The difference soil surface albedo with different vegetation cover was significant large, as Gu et al., found that the surface albedo under lower of 30% vegetation cover was about 1.7 times that under the 93% vegetation cover (Gu et al., 2005). Therefore, the net radiation  $R_n$  varied with different vegetation cover level. The  $R_n$  under 93% vegetation cover exceeds those of 30% vegetation cover by 16–20% (Ma et al., 2006). The differences of heat transmission and surface heat flux under different vegetation cover were related to the different heat balance and heat consumed level. The variation of heat balance and soil surface heat flux entered into or leaved from soil was significant with different vegetation cover and in different season. That was the main factor to cause the variation of the soil-air temperature difference and soil temperature under different vegetation cover.

The soil organic matter content, particle size and distribution have significant effect on permafrost soil heat capacity and conductivity (Zhou et al., 2000). As the vegetation cover upon the studied alpine meadow decreased due to degradation, the content of coarse grains in the surface soil layer increased, organic matter content decreased, soil heat conductivity and heat capacity were correspondingly enhanced, and an increase in the heat content of the deep soil layer led to an increase in the thawing depth. Given that the vegetation cover of alpine meadow in the study region is proportional to the content of organic matter within the soil (Wang et al., 2001a; Zhou, 2001), the higher the vegetation cover have, the smaller the amplitude of soil temperature changes with

## Impacts of vegetation cover on soil water heat regime

W. Genxu et al.

Title Page

Abstract

Introduction

Conclusions

References

Tables

Figures

◀

▶

◀

▶

Back

Close

Full Screen / Esc

Printer-friendly Version

Interactive Discussion



time and the larger the soil-air temperature difference.

In permafrost region, the heat transmission and soil temperature gradient controlled the soil profile distribution during freezing and thawing periods (Zhou et al., 2000; Zhang et al., 2003). Soil freezing and thawing temperatures are related to soil moisture content, grain size composition, soil structure, and organic matter content; these soil properties vary with changes in vegetation cover. Thus, the influences of changes in vegetation cover on the soil water and heat coupling regimes of an alpine meadow are manifest in two ways: first, vegetation directly affects the transmission of water and heat; second, vegetation indirectly affects the transmission of water and heat via changes in the physical properties of the soil.

## 6 Conclusions

Degradation of the alpine meadow resulted in a reduction in the depth of soil freezing, an increase in the soil thawing temperature, and a tighter response of  $T_s$  to changes in  $T_a$ . The surface heat flux and soil heat storage in the upper 20 cm layer increased with increasing vegetation cover, while the downward transmitted heat flux decreased. The greater the vegetation cover, the greater the heat-insulating effect of the surface soil layer, which acted to reduce both the upward heat flux during the period of frozen soil and the downward heat flux during the thawing period. This finding indicates that healthy vegetation within alpine meadows in the permafrost region provides excellent heat insulation. The maintenance of a high vegetation cover upon alpine meadows is favourable to slowing the heat cycling of the permafrost and minimizing the impact of climate change on the permafrost. Hence, protection of alpine meadows is important in maintaining the stability of engineering works constructed within frozen soil upon the Qinghai-Tibet Plateau.

Changes in vegetation coverage upon the studied alpine meadow had a significant affect on the coupling of  $\theta_v$  and  $T_s$ . When the vegetation of such meadows is degraded and vegetation cover reduced, clear changes are observed in the  $\theta_v$ - $T_s$  relationship.

## Impacts of vegetation cover on soil water heat regime

W. Genxu et al.

Title Page

Abstract

Introduction

Conclusions

References

Tables

Figures

◀

▶

◀

▶

Back

Close

Full Screen / Esc

Printer-friendly Version

Interactive Discussion



For a given  $T_s$ ,  $\theta_v$  increased with increasing vegetation cover. Alpine meadow soils under a high vegetation cover exhibit a high water-storage capacity during the freezing period; this water clearly accumulates in the root zone (0–0.20 m) during the thawing period, thereby favoring the growth of vegetation in alpine meadows.

- 5 *Acknowledgements.* This study was funded by the national key scientific plan (973) (No. 2007CB411504), the Natural Science Foundation of China (No. 40730634) and the grant awarded to Wang Genxu under the auspices of the “Hundred People” Project of the Chinese Academy of Sciences.

## References

- 10 Bubier, J. L., Frohling, S., Crill, P. M., and Linder, E.: Net ecosystem productivity and its uncertainty in a diverse boreal peatland, *J. Geophys. Res.*, 104(D22), 27 683–27 693, 1999.
- Carey, S. K. and Woo, M. K.: Hydrology of two slopes in subarctic Yukon, Canada, *Hydrol. Process*, 13, 2549–2562, 1999.
- Cheng, G.: Problems on zonation of high altitude permafrost, *Acta Geogr. Sin.*, 39(2), 185–193, 1984.
- 15 Chen, R., Lu, S., and Kang, E.: A distributed water-heat coupled (DWHC) model for mountainous watershed: model structure and equations, *Advances in Earth Science*, 21(8), 806–818, 2006.
- Christensen, T. R., Johansson, T., and Kerman, H. J.: Thawing sub-arctic permafrost: effects on vegetation and methane emissions, *Geophys. Res. Lett.*, 31, L04501, doi:10.1029/2003GL018608, 2004.
- 20 Flerchinger, G. N.: The Simultaneous Heat and Water (SHAW) Model: User’s Manual, Technical Report NWRC 2000-10, Northwest Watershed Research Center, 2000.
- Eugster, W., Rouse, W., Pielkes, R. A., Mcfadden, J. P., Baldocchi, D. D., Kittel, T. G. F., Chapin, F. S., Liston, G. E., Vidale, P. L., Vaganov, E., and Chambers, S.: Land-atmosphere energy exchange in Arctic tundra and boreal forest: available data and feedbacks to climate, *Global Change Biol.*, 6, 84–115, 2000.
- 25 Jansson, P.-E. and Karlberg, L.: COUP manual Coupled heat and mass transfer model for soil-

## Impacts of vegetation cover on soil water heat regime

W. Genxu et al.

Title Page

Abstract

Introduction

Conclusions

References

Tables

Figures

◀

▶

◀

▶

Back

Close

Full Screen / Esc

Printer-friendly Version

Interactive Discussion



plant-atmosphere systems, 2001, available at: <http://www.lwr.kth.se/Vara%20Datorprogram/CoupModel/index.htm>, 2001.

Jorgenson, M. T., Racine, C. H., and Walters, J. C.: Permafrost degradation and ecological changes associated with a warming in central Alaska, *Clim. Change*, 48, 551–579, 2001.

5 Kang, E., Cheng, G., and Song, K.: Simulation of energy and water balance in Soil-Vegetation-Atmosphere Transfer system in the mountain area of Heihe river basin, China, *Sci. China Ser. D.*, 48(4), 538–548, 2005.

Legates, D. R. and McCabe, G. J.: Evaluating the use of “goodness-of-fit” measures in hydrologic and hydro-climatic model validation, *Water Resour. Res.*, 35(1), 233–241, 1999.

10 Ma, Y., Yao, T., Wang, J., and Hu, Z.: The Study on the Land Surface Heat Fluxes over Heterogeneous Landscape of the Tibetan Plateau, *Adv. Earth Sci.*, 21(12), 1215–1224, 2006.

McGuire, A. D.: Environmental variation, vegetation distribution, carbon dynamics and water/energy exchange at high latitudes, *J. Veg. Sci.*, 13(1), 301–314, 2002.

Mayocchi, C. L. and Bristowa, K. L.: Soil surface heat flux: some general questions and comments on measurements, *Agricultural and Forest Meteorology*, 75, 43–50, 1995.

Ministry of Agriculture of China: Technical specifications of soil analysis, Chinese Agriculture Press, Beijing, China, 14–172, 1993.

Nash, J. E. and Sutcliffe, J. V.: River flow forecasting through conceptual models, 1, discussion of principles, *J. Hydrol.*, 10, 282–292, 1970.

20 National Soil Survey Office (NSSO): Soil of China, Chinese Agriculture Press, Beijing, China, 1998.

NWRC: SHAW (Vol.2.3.6.), available at: <http://www.nwrc.ars.usda.gov/SP2userfiles/Place/53620000/shaw>, 2004.

25 Oechel, W. C., Vourlitis, G. L., Hastings, S. J., Zulueta, R. C., Hinzman, L., and Kane, D.: Acclimation of ecosystem CO<sub>2</sub> exchange in the Alaskan Arctic in response to decadal climate warming, *Nature*, 406, 978–980, 2000.

Payero, J. O., Eale, C. M. U., Wright, J. L., and Allen, R. G.: Guidelines for validating Bowen Ratio data, *T. ASAE*, 46(4), 1051–1060, 2003.

30 Rouse, W. R.: Progress in hydrological research in the Mackenzie GEWEX study, *Hydrol. Process.*, 14, 1667–1685, 2000.

Smith, M. W. and Riseborough D. W.: Ground temperature monitoring and detection of climate change, *Permafrost Periglac.*, 7(4), 301–310, 1996.

Smith, M. W. and Riseborough, D. W.: Climate and the limits of permafrost: a zonal analysis,

# HESSD

5, 2543–2579, 2008

---

## Impacts of vegetation cover on soil water heat regime

W. Genxu et al.

---

Title Page

Abstract

Introduction

Conclusions

References

Tables

Figures

◀

▶

◀

▶

Back

Close

Full Screen / Esc

Printer-friendly Version

Interactive Discussion



- Permafrost Periglac., 13(1), 1–15, 2002.
- Gu, S., Tang, Y. H., Cui, X. Y., Kato, T., Du, M. Y., Li, Y. N., and Zhao, X. Q.: Energy exchange between the atmosphere and a meadow ecosystem on the Qinghai-Tibetan Plateau, *Agr. Forest Meteorol.*, 129, 175–185, 2005.
- 5 Turetsky, M. R., Kelman Wieder, R., and Vitt, D. H.: Boreal peatland C fluxes under varying permafrost regimes, *Soil Biol. Biochem.*, 34, 907–912, 2002.
- Walker, D. A., Jia, G. J., and Epstein, H. E.: Vegetation-soil-thaw-depth relationships along a low-arctic bioclimate gradient, Alaska: synthesis of information from the ATLAS studies, *Permafrost Periglac.*, 14, 103–123, 2003.
- 10 Wang G., Li, Q., Cheng, G., and Shen, Y.: Climate change and its impact on the eco-environment in the source regions of Yangtze and Yellow Rivers in recent 40 years, *Journal of Glaciology and Geocryology*, 23(4), 346–352, 2001a.
- Wang, G., Cheng, G. D., Shen, Y. P., et al.: Research on ecological environmental changes in Yangtze and Yellow Rivers source regions and their integrated protection, Lanzhou University Press, Lanzhou, China, 213 pp., 2001b (in Chinese).
- 15 Wang, G., Ding, Y., Wang, J., and Liu, S.: Land ecological changes and evolutionary patterns in the source regions of the Yangtze and Yellow Rivers, *Acta Geogr. Sin.*, 15(2), 163–173, 2004.
- Weller, G., Chapin, F. S., Everett, K. R., and Hobbie, J. E.: The arctic FLUX study: a regional view of gas release, *J. Biogeogr.*, 22, 365–374, 1995.
- 20 Wu, Q. and Liu, Y.: Ground temperature monitoring and its recent change in Qinghai-Tibet Plateau, *Cold Reg. Sci. Technol.*, 38, 85–92, 2004.
- Wu, Q. B., Shi, B., and Liu, Y. Z.: Research on the interaction of permafrost and highway along Qinghai-Tiber highway, *Sci. China Ser. D.*, 32(6), 514–520, 2002.
- 25 Xu, X., Wang, J., and Zhang, L.: Permafrost physics, Science Press, Beijing, China, 310 pp., 2001 (in Chinese).
- Zhang, Y., Ohata, T., and Kadata, T.: Land surface hydrological processes in the permafrost region of the eastern Tibetan Plateau, *J. Hydrol.*, 283, 41–56, 2003.
- Zhou, Y., Guo, D., Qiu, G., and Cheng, G.: *Geocryology in China*, Science Press, Beijing, China, 450 pp., 2000 (in Chinese).
- 30 Zhou, X. M.: *Chinese Kobresia pygmaea meadow*, Science Press, Beijing, China, 370 pp., 2001 (in Chinese).

---

**Impacts of vegetation cover on soil water heat regime**W. Genxu et al.

---

[Title Page](#)[Abstract](#)[Introduction](#)[Conclusions](#)[References](#)[Tables](#)[Figures](#)[◀](#)[▶](#)[◀](#)[▶](#)[Back](#)[Close](#)[Full Screen / Esc](#)[Printer-friendly Version](#)[Interactive Discussion](#)

## Impacts of vegetation cover on soil water heat regime

W. Genxu et al.

**Table 1.** Physical and chemical characteristics of selected alpine meadow soils of the Qinghai-Tibet Plateau.

Type	Vegetation type Cover (%)	Permafrost		Soil Profile (m)	Bulk density (Mg m <sup>-3</sup> )	Granularity		Organic matter (%)
		Depth (m)	Active layer (m)			>0.5 mm (%)	<0.1 mm (%)	
<i>Festuca</i> sp., <i>Poa</i> spp.	30	50–120	1.0–1.5	0–0.10	1.26	4.95	93.1	0.66
				0.10–0.20	1.34	11.3	85.4	0.25
				0.20–0.40	1.51	17.95	61.2	1.13
<i>Kobresia humilis</i>	65	50–120	0.8–1.5	0–0.10	1.10	1.45	93.2	1.30
				0.10–0.20	1.21	2.85	92.9	0.80
				0.20–0.40	1.35	7.2	72.4	0.77
<i>Kobresia humilis</i>	93	50–120	0.8–1.5	0–0.10	0.95	1.15	93.3	1.10
				0.10–0.20	1.09	1.6	93.6	1.63
				0.20–0.40	1.29	11.65	61.8	1.38

Title Page

Abstract

Introduction

Conclusions

References

Tables

Figures

◀

▶

◀

▶

Back

Close

Full Screen / Esc

Printer-friendly Version

Interactive Discussion



## Impacts of vegetation cover on soil water heat regime

W. Genxu et al.

**Table 2.** Soil heat content and its distribution in the soil profile of alpine meadow soils of the Qinghai-Tibet Plateau under different levels of vegetation cover.

Vegetation cover	Soil freezing period kJ/m <sup>2</sup>				Soil thawing period kJ/m <sup>2</sup>			
	20 cm	40 cm	70 cm	120 cm	20 cm	40 cm	70 cm	120 cm
65%	-57.37	-97.54	-42.18	-11.53	39.89	67.91	60.80	3.79
93%	-26.05	-91.78	-34.23	-11.06	29.60	50.80	56.95	2.60
30%	-99.61	-140.19	-93.70	-15.44	53.20	69.80	96.89	5.70

Title Page

Abstract

Introduction

Conclusions

References

Tables

Figures

◀

▶

◀

▶

Back

Close

Full Screen / Esc

Printer-friendly Version

Interactive Discussion



**Impacts of vegetation cover on soil water heat regime**

W. Genxu et al.

**Table 3.** Regression models of the relationship between the soil moisture content ( $\theta_v$ ) and soil temperature ( $T_s$ ) of alpine meadow soils of the Qinghai-Tibet Plateau under different levels of cover and during the freezing and thawing periods.

Period	Vegetation cover (%)	Models relating $T_s$ and $\theta_v$	Correlation coefficient, $R$	Relative error (%)	Standard error (%)
Freezing	93%	$T_s = -9.24 + 9.0 / (1 + \exp[-(\theta_v - 13.05)/0.74])$	0.97	0.15	0.45
	65%	$T_s = -275.3 + 274.9 / (1 + \exp[-(\theta_v + 0.48)/1.47])$	0.98	0.30	0.51
	30%	$T_s = -78.2 + 78.1 / (1 + \exp[-(\theta_v - 2.93)/1.51])$	0.94	0.43	0.58
Thawing	93%	$T_s = -1.16 + (0.46 \times \ln (\theta_v - 13.86) )$	0.91	2.5	0.38
	65%	$T_s = -0.96 + (0.50 \times \ln (\theta_v - 5.94) )$	0.88	6.1	0.41
	30%	$T_s = -1.02 \times \theta_v / (-4.15 + \theta_v) + 0.115 \times \theta_v$	0.93	0.5	0.43

Note:  $T_s$ , soil temperature;  $\theta_v$ , volumetric soil moisture.

Title Page

Abstract Introduction

Conclusions References

Tables Figures

◀ ▶

◀ ▶

Back Close

Full Screen / Esc

Printer-friendly Version

Interactive Discussion



## Impacts of vegetation cover on soil water heat regime

W. Genxu et al.

**Table 4.** Accuracy of the simulated soil heat content of alpine meadow soils of the Qinghai-Tibet Plateau under different levels of vegetation cover.

Period	Percent cover					
	93%		65%		30%	
	<i>RE%</i>	<i>NSE%</i>	<i>RE%</i>	<i>NSE%</i>	<i>RE%</i>	<i>NSE%</i>
Freezing	21.4	61.3	13.5	86.4	19.1	90.3
Thawing	2.1	75.3	20.0	83.5	12.5	87.1

Note: *RE*, relative error; *NSE*, Nash-Sutcliffe coefficient of efficiency.

Title Page

Abstract

Introduction

Conclusions

References

Tables

Figures

◀

▶

◀

▶

Back

Close

Full Screen / Esc

Printer-friendly Version

Interactive Discussion



## Impacts of vegetation cover on soil water heat regime

W. Genxu et al.

**Table 5.** Comparison of the mean soil–air temperature difference ( $\Delta\bar{T}_{a-s}$ ), soil freezing temperature ( $^fT_s$ ), and soil thawing temperature ( $^tT_s$ ) of alpine meadow soils of the Qinghai-Tibet Plateau under different levels of vegetation cover.

Vegetative cover	Freezing period			Thawing period			Warm season	
	Slope	$\Delta\bar{T}_{a-s}$	$^fT_s$	Slope	$\Delta\bar{T}_{a-s}$	$^tT_s$	Slope	$\Delta\bar{T}_{a-s}$
93%	0.66	−3.5	−0.10	0.86	6.0	0.04	1.02	4.5
65%	0.55	−2.4	−0.78	0.83	5.5	0.3	0.95	4.2
30%	0.52	−2.0	−1.77	0.71	4.4	1.74	0.86	3.5

Title Page

Abstract

Introduction

Conclusions

References

Tables

Figures

◀

▶

◀

▶

Back

Close

Full Screen / Esc

Printer-friendly Version

Interactive Discussion



## Impacts of vegetation cover on soil water heat regime

W. Genxu et al.

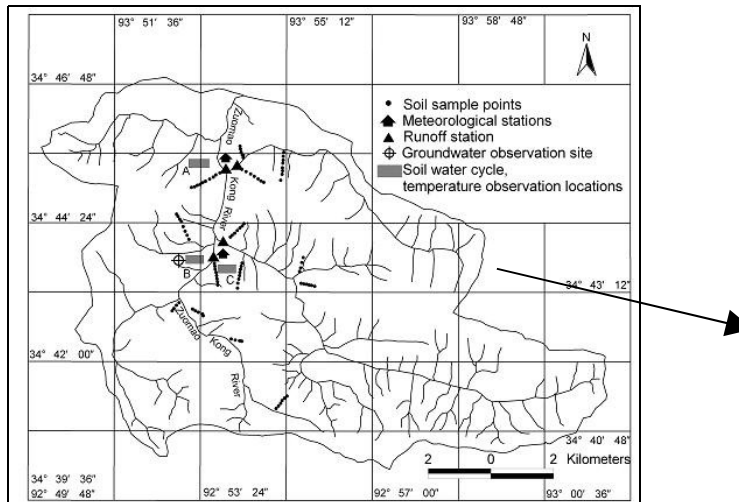


Fig. 1. Location map of the study area.

Title Page

Abstract

Introduction

Conclusions

References

Tables

Figures



Back

Close

Full Screen / Esc

Printer-friendly Version

Interactive Discussion



Impacts of vegetation cover on soil water heat regime

W. Genxu et al.

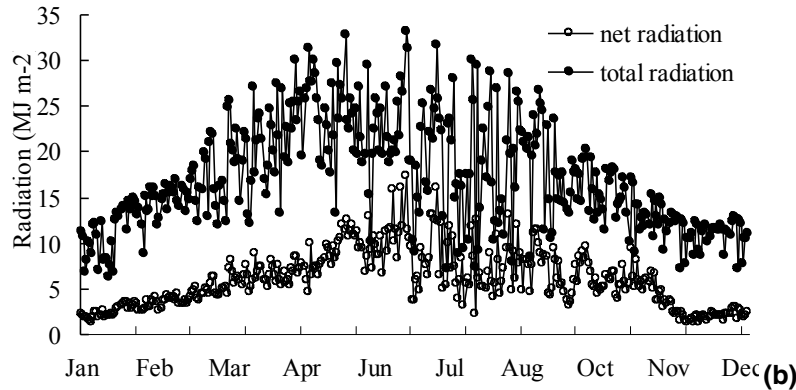
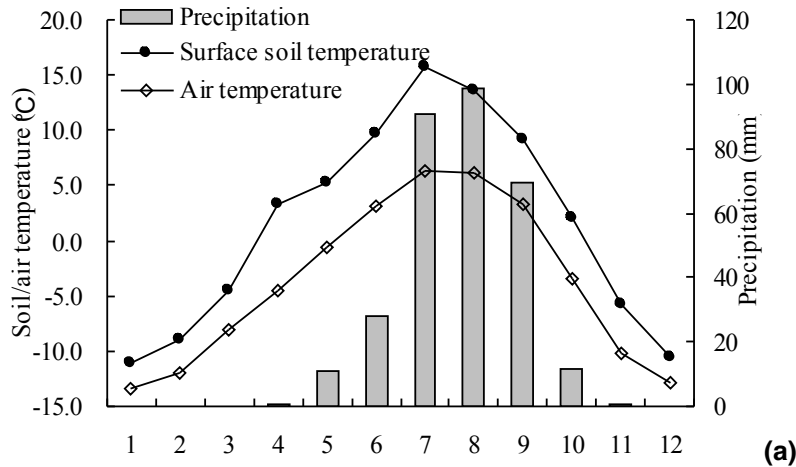


Fig. 2. Monthly precipitation, air temperature and soil temperature at 5 cm depth (a); Monthly total radiation and net radiation (b).

- Title Page
- Abstract Introduction
- Conclusions References
- Tables Figures
- Navigation: Left Arrow, Right Arrow, Double Left Arrow, Double Right Arrow
- Back Close
- Full Screen / Esc
- Printer-friendly Version
- Interactive Discussion



## Impacts of vegetation cover on soil water heat regime

W. Genxu et al.

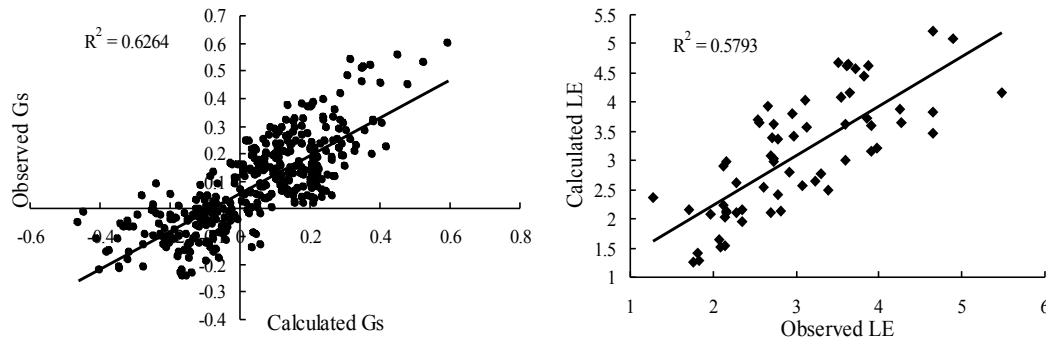


**Fig. 3.** The comparison of calculated  $G_s$  with observed  $G_s$  (a), and calculated  $LE$  with the observed  $LE$  (b).

Title Page

Abstract

Introduction

Conclusions

References

Tables

Figures

◀

▶

◀

▶

Back

Close

Full Screen / Esc

Printer-friendly Version

Interactive Discussion



## Impacts of vegetation cover on soil water heat regime

W. Genxu et al.

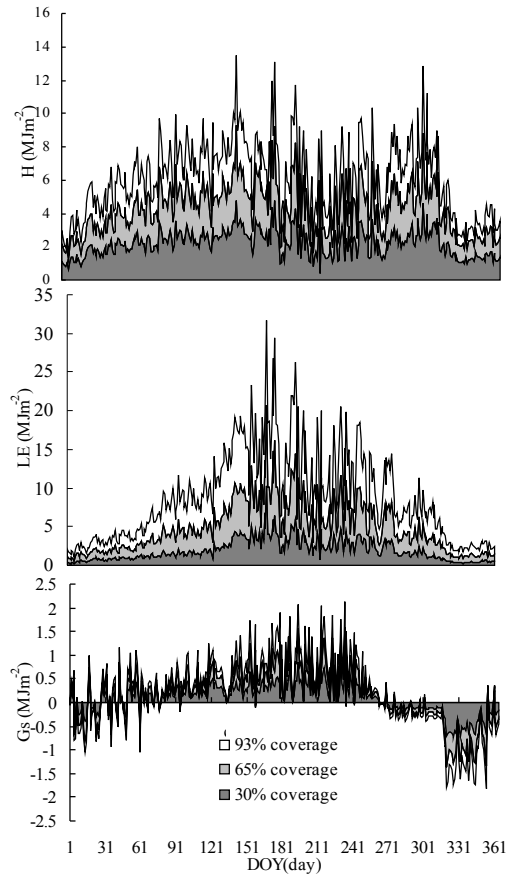


**Fig. 4.** Seasonal variations of daily-integrated sensible heat flux ( $H$ ), latent heat flux ( $LE$ ), and soil heat flux ( $G_s$ ).

Title Page

Abstract

Introduction

Conclusions

References

Tables

Figures

◀

▶

◀

▶

Back

Close

Full Screen / Esc

Printer-friendly Version

Interactive Discussion



Impacts of vegetation cover on soil water heat regime

W. Genxu et al.

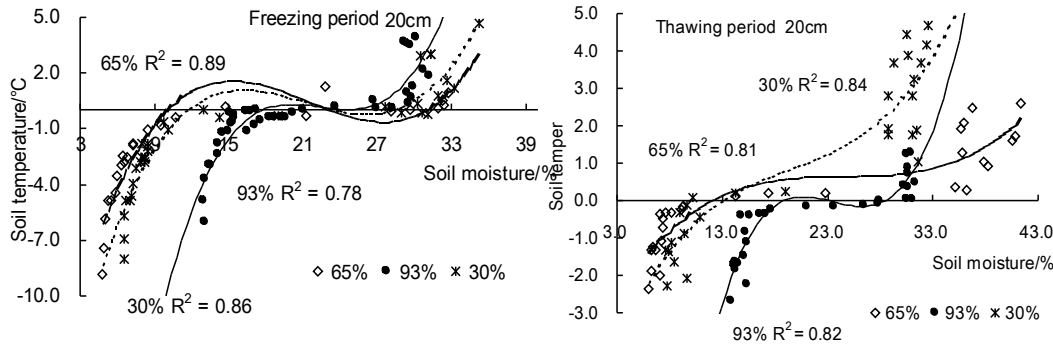


**Fig. 5.** Relationship between soil moisture content ( $\theta_v$ ) and soil temperature ( $T_s$ ) for alpine meadow soils of the Qinghai-Tibet Plateau. Data are plotted for different levels of vegetation cover during the freezing and thawing periods at 20 cm depth.

Title Page

Abstract

Introduction

Conclusions

References

Tables

Figures

◀

▶

◀

▶

Back

Close

Full Screen / Esc

Printer-friendly Version

Interactive Discussion



Impacts of vegetation cover on soil water heat regime

W. Genxu et al.

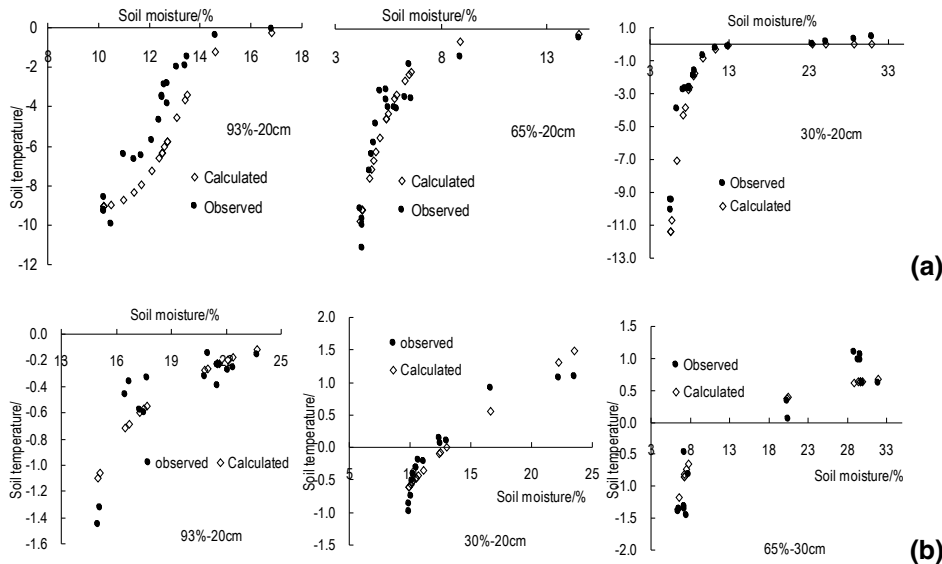


**Fig. 6.** Comparison of  $\theta_v-T_s$  coupling based on predicted and observed  $T_s$  during freezing periods **(a)** and thawing periods **(b)**.

Title Page

Abstract

Introduction

Conclusions

References

Tables

Figures

◀

▶

◀

▶

Back

Close

Full Screen / Esc

Printer-friendly Version

Interactive Discussion



Impacts of vegetation cover on soil water heat regime

W. Genxu et al.

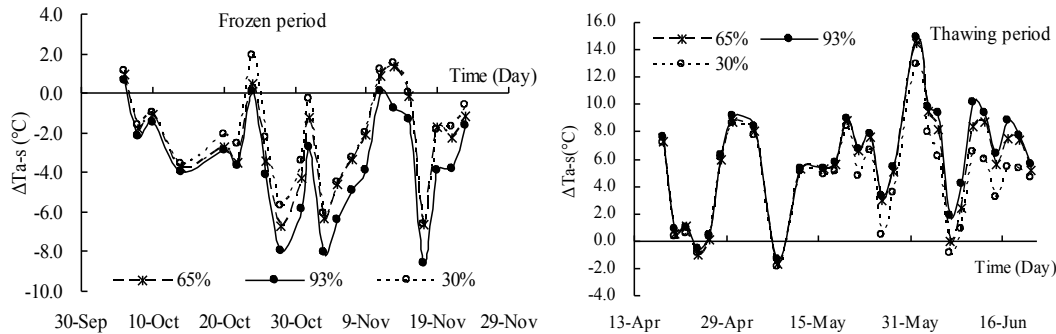


**Fig. 7.** Relationship between the soil–air temperature difference ( $\Delta T_{a-s}$ ) and air temperature ( $T_a$ ) at 20 cm depth during freezing periods and thawing periods for the studied alpine meadow soils under different levels of vegetation cover.

Title Page

Abstract

Introduction

Conclusions

References

Tables

Figures

◀

▶

◀

▶

Back

Close

Full Screen / Esc

Printer-friendly Version

Interactive Discussion



Impacts of vegetation cover on soil water heat regime

W. Genxu et al.

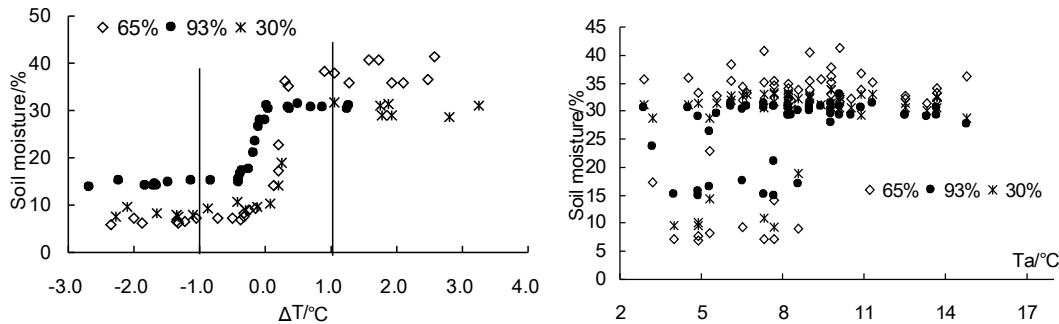


**Fig. 8.** Relationship between the soil–air temperature difference ( $\Delta T_{a-s}$ ) and soil moisture content ( $\theta_v$ ) for alpine meadow soils of the Qinghai-Tibet Plateau under different levels of vegetation cover.

Title Page

Abstract Introduction

Conclusions References

Tables Figures

◀ ▶

◀ ▶

Back Close

Full Screen / Esc

Printer-friendly Version

Interactive Discussion



Impacts of vegetation cover on soil water heat regime

W. Genxu et al.

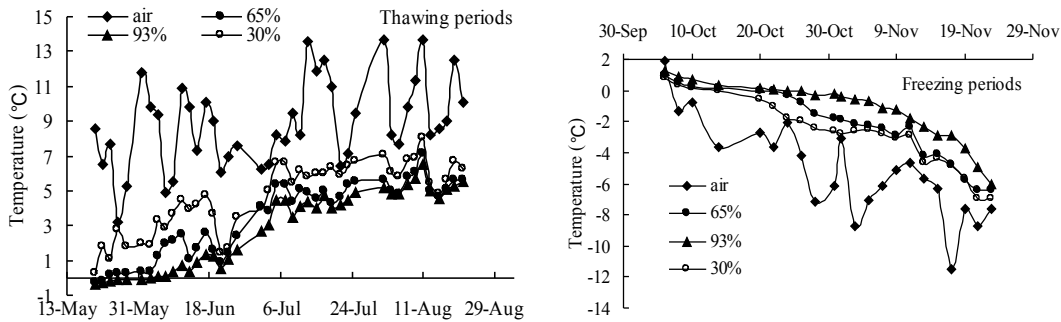


**Fig. 9.** Dynamic changes in soil temperature with air temperature measured in the 0–20 layer under different levels of vegetation cover during the thawing period and freezing period.

Title Page

Abstract

Introduction

Conclusions

References

Tables

Figures

◀

▶

◀

▶

Back

Close

Full Screen / Esc

Printer-friendly Version

Interactive Discussion

